

¹³C NMR Spectroscopy of ¹³C₁-Labeled Octanethiol-Protected Au Nanoparticles: Shifts, Relaxations, and Particle-Size Effect

Brian S. Zelakiewicz, Angel C. de Dios, and YuYe Tong*

Department of Chemistry, Georgetown University, 37th and "O" Streets NW, Washington, DC 20057

Received August 27, 2002; E-mail: yyt@georgetown.edu

The potential technical importance of monolayer-protected metal nanoparticles in developing nanoscale (opto)electronic devices, (bio)chemical sensors, corrosion-resistant materials, and new catalysts has made them one of the primary targets of the most intensive research during the past decade,¹ in particular after Brust and co-workers' seminal work on the two-phase synthesis of alkanethiol-protected Au nanoparticles.² Two fundamental aspects of particular current interest are the three-dimensional quantum confinement of electrons³ and the metal–ligand interaction,⁴ and it is, therefore, highly desirable to develop techniques that enable detailed investigations of these fundamental aspects. Both liquid ¹H^{5,6} and liquid/solid-state ¹³C^{7–9} NMR have been previously used to characterize the alkanethiol-protected Au nanoparticles. However, although intuitively expected, no particle-size effect on any NMR observables of the most proximal carbon to the Au surface, C₁, has ever been reported thus far. In this communication, we report the first observations of such an important particle-size effect on the NMR observables of C₁. It demonstrates that the ¹³C NMR of the protecting, C₁-labeled octanethiol (or alkanethiol in general) is indeed a sensitive function of the underlying particle size, therefore, is promising to be used as a powerful microscopic probe to investigate in detail the effect of the quantum confinement and the metal–ligand interaction.

Octanethiol-protected Au nanoparticles were prepared by the well-established two-phase approach. Five samples with Au/¹³C₁-labeled octanethiol (Isotech, Miamisburg, OH) ratio of respectively 1:5, 2:1, 5:1, 7:1, and 10:1 were so-prepared. The TEM data of good quality are obtained for all but the 1:5 samples. The average particle sizes so-measured are 2.1 ± 0.3, 2.8 ± 0.6, 3.8 ± 0.9, and 4.0 ± 1.1 nm respectively, with an overwhelming majority of particles showing a spherical form. An estimate of particle size, 1.6 nm, was obtained for the 1:5 sample using an electrochemical quantized double-layer charging/discharging technique. The cleanliness of the final products was always checked by the standard ¹H and ¹³C solution NMR in C₆D₆ (Cambridge Isotope, Andover, MA) on a Varian Unity 500 MHz spectrometer.

All NMR measurements reported here were carried out at room temperature on a "home-assembled" 400-MHz spectrometer equipped with an Oxford active-shielded 9.395-T widebore superconducting magnet and a Tecmag Libra acquisition system. The NMR sample consisted of the concentrated C₆D₆ solution of Au nanoparticles flame-sealed into a 10 mm × 25 mm glass ampule. A Hahn spin-echo pulse sequence ($\pi/2 - \tau_0 - \pi - \tau_0 - \text{acq.}$) with phase cycling was used for data acquisition. The $\pi/2$ pulse = 6 s and $\tau_0 = 50$ s. The chemical shift of C₆D₆ (128.39 ppm with respect to TMS) was used as the internal secondary reference. The T_1 's were measured by conventional inversion–recovery method and the T_2 's by monitoring the spectral amplitude as a function of τ_0 in the Hahn echo sequence. All repetition times were set to 5 T_1 .

We show in Figure 1A the ¹³C NMR spectra of ¹³C₁-labeled octanethiol on 1.6 (black), 2.1 (red), 2.8 (blue), 3.8 (dark violet),

and 4.0 nm (cyan) Au samples. The remarkable observation here is that, although the spectra are quite broad, their positions are clearly a function of the particle size. The bigger the particle size is, the more positive is the shift which approaches an apparent limiting value. This is graphically shown in Figure 1B in which the center of gravity of the spectrum is plotted against the particle size (solid circles). Two interpretations are most plausible. The first one is the surface coordination effect, that is, the Au–thiol bonding, therefore, the ¹³C₁ NMR shift, is directly influenced by the coordination number (CN) of a surface atom at which the bonding takes place. Approximating the Au nanoparticles by a fcc cubo-octahedron of the size equal to the average particle diameter of the sample, one can easily express analytically¹⁰ the fraction of the high CN terrace surface sites, x , as a function of the particle diameter, d . The fraction of the remaining low CN corner and edge sites is thus $1 - x$. Assuming now that the center of gravity of the spectra traces the average value of the two limiting cases, that is $\delta = x\delta_{\text{terrace}} + (1 - x)\delta_{\text{corner}}$, where δ_{terrace} and δ_{corner} are respective shifts of thiols bound to particles having d approaching zero and infinite, we obtained an excellent fit as shown by the solid curve in Figure 1B, with $\delta_{\text{terrace}} = 61$ ppm and $\delta_{\text{corner}} = 27$ ppm. Note that the ¹³C₁ shift in Au(I)SC₄H₉ and Au(I)SC₁₄H₂₉ complexes is 40.1 ppm⁹ and that those of alkyl species adsorbed on silica-supported Ru catalyst are between 12 and 35 ppm.¹¹ However, no data exist for thiols on bulk Au surfaces.

The second plausible interpretation is the quantum size effect that affects the Au–thiol bonding, and consequently, the ¹³C₁ NMR shift as particle size changes. While a quantitative expression is currently lacking, a qualitative rationale in terms of work function can still be put forward. In a jellium model, the work function of a metal particle, W , can be expressed as $W_{\text{bulk}} + 2c/d$ where W_{bulk} is the work function of the bulk and c is the quantum correction.¹² The asymptotic form of the spillover electron density outside the metal surface is proportional to $\exp(-2z\sqrt{2W})$ where z is the normal distance from the surface.¹³ Thus, if the spillover electron density is a measure of the ability of a metal surface to bind ligands, then the ¹³C₁ NMR shift is expected to be a function of the particle size and approach a limiting value, as observed here. Clearly, more investigations are needed to discern these two interpretations. Nonetheless, in both cases the variation in ¹³C₁ NMR shift is rationalized as a result of the changes in the Au–thiol bonding due to changes in the electronic properties of the underlying Au nanoparticles. In addition, the ¹³C₁ shifts observed here are in general more positive than those of the Au–thiol complexes⁹ and the alkyl species on Ru.¹¹ Thus, the variation in the ¹³C₁ shift may well come from the Knight shift.

The main objection to a Knight-shift interpretation comes from the fact that no Korringa relationship has been observed for the spin–lattice relaxation rate as a function of temperature.⁹ However, since the Knight shift contribution, if any, is quite small (\leq tens ppm), the Korringa mechanism is therefore not expected to be the

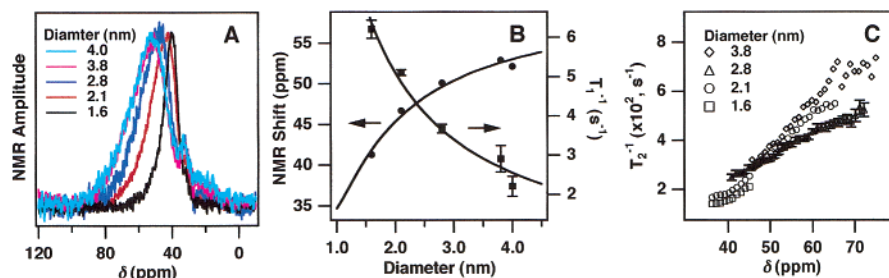


Figure 1. (A) ¹³C NMR spectra of ¹³C-labeled octanethiol-protected Au nanoparticles prepared with different particle sizes: 1.6 (black), 2.1 (red), 2.8 (blue), 3.8 (dark violet), and 4.0 nm (cyan). Spectra were recorded at room temperature. The typical number of scans was 3200. A line broadening of 25 Hz was used for all spectra. (B) Particle size dependence of the ¹³C NMR spectral center of gravity (solid circles, left axis) and the spin–lattice relaxation rate T_1^{-1} (solid squares, right axis). Solid curves are fits to the surface coordination and random Brownian motion models respectively (see the text for details). (C) Across-the-spectrum spin–spin relaxation rate data for samples of size 1.6 (squares), 2.1 (circles), 2.8 (triangles with representative error bars), and 3.8 nm (diamonds).

dominant relaxation channel. Indeed, for ¹³C, the Korringa expression¹⁴ for the spin–lattice relaxation rate is $T_1^{-1} = 2.4 \times 10^5 TK^2$ (s⁻¹) where T is the absolute temperature (for our case $T = 300$ K) and K is the Knight shift. For a Knight shift of 12 ppm (the order of the variation observed), the associated spin–lattice relaxation rate would be 0.01 s⁻¹. As also shown in Figure 1B (solid squares), the T_1^{-1} 's measured at the peak positions are at least 200 times faster than the possible Korringa contribution estimated above. Thus, it is not surprising that particle-size dependence of the T_1^{-1} goes in a direction against that of the NMR shift and decreases monotonically as the particle size increases. Using the Einstein–Smoluchowski and Stoke–Einstein equations for random Brownian motion in solution¹⁵ and assuming a “strong-collision” limit¹⁴ for the relaxation, one can find that $T_1^{-1} = \text{Constant}/d$, which (the corresponding fitting curve in Figure 1B) describes very well the experimental results. Thus, we are confident that the same dominant spin–lattice relaxation channel, that is, the random motion-induced relaxation, is active for all C₁'s regardless of the distribution of local chemical environment. Detailed temperature-dependent studies should provide more insightful information.

The results of spin–spin relaxation rate (T_2^{-1}) measurements on four samples are presented in Figure 1C. Unlike T_1^{-1} , the T_2^{-1} shows a ubiquitous across-the-spectrum variation. Such a behavior is in agreement with the previous hole-burning experiment,⁹ indicating that even in the liquid state the NMR line is heterogeneously and asymmetrically broadened, due primarily to distributions of the chemical environment (such as Au–thiol bonding) and particle size. T_2^{-1} is also 2 orders of magnitude larger than T_1^{-1} , very similar to the situations usually observed in solid state, but still much slower than the solid-state ¹³C–¹H heteronuclear dipolar dephasing.⁸ This suggests that the modulation of the local field as seen by C₁ is fast enough to push the spin–spin relaxation into the “weak-collision” limit.¹⁴ Finally, similar to the NMR shift and T_1^{-1} , the T_2^{-1} shows a clear particle-size dependence.

In summary, we have shown for the first time that the three major NMR observables (shift, T_1^{-1} , and T_2^{-1}) of the proximal ¹³C₁ in the protecting octanethiol ligand (or alkanethiol in general) are sensitive functions of the size of the underlying Au nanoparticles.

These observations are of general interest for at least two main reasons. First, it opens the way for more widespread applications of this simple yet versatile ¹³C₁ NMR spectroscopy to investigate in detail the effect of quantum confinement and metal–ligand interactions in diverse monolayer-protected nanosystems. Second, the experimental results so obtained will provide an exceptional arena for advanced quantum chemistry investigations.

Acknowledgment. We are grateful to Professor G. Chapman for TEM measurement assistance. The work is partially supported by the Georgetown Graduate School Pilot Research Project Grant, the startup as well as the PRF fund (to Y.Y.T.), and the NSF CAREER Award and the PRF fund (to A.C.D.).

References

- (1) Feldheim, D. L.; Foss, C. A., Jr., Eds. *Metal Nanoparticles*; Marcel Dekker: New York, 2002.
- (2) Brust, M.; Walker, M.; Bethell, D.; Schiffrin, D. J.; Whyman, R. *J. Chem. Soc., Chem. Commun.* **1994**, 801–802.
- (3) Markovich, G.; Collier, C. P.; Henrichs, S. E.; Remacle, F.; Levine, R. D.; Heath, J. R. *Acc. Chem. Res.* **1999**, *32*, 415–423.
- (4) Gronbeck, H.; Curioni, A.; Andreoni, W. *J. Am. Chem. Soc.* **2000**, *122*, 3839–3842.
- (5) Hostetler, M. J.; Wingate, J. E.; Zhong, C.-J.; Harris, J. E.; Vachet, R. W.; Clark, M. R.; Londono, J. D.; Green, S. J.; Stokes, J. J.; Wignall, G. D.; Glish, G. L.; Porter, M. D.; Evans, N. D.; Murray, R. W. *Langmuir* **1998**, *14*, 17–30.
- (6) Hasan, M.; Bethell, D.; Brust, M. *J. Am. Chem. Soc.* **2002**, *124*, 1132–1133.
- (7) Terrill, R. H.; Postlethwaite, T. A.; Chen, C.-H.; Poon, C.-D.; Terzis, A.; Chen, A.-D.; Hutchinson, J. E.; Clark, M. R.; Wignall, G.; Londono, J. D.; Superfine, R.; Falvo, M.; Johnson, C. S., Jr.; Samulski, E. T.; Murray, R. W. *J. Am. Chem. Soc.* **1995**, *117*, 12537–12548.
- (8) Badia, A.; Gao, W.; Singh, S.; Demers, L.; Cuccia, L.; Reven, L. *Langmuir* **1996**, *12*, 1262–1269.
- (9) Badia, A.; Demers, L.; Dickinson, L.; Morin, F. G.; Lennox, R. B.; Reven, L. *J. Am. Chem. Soc.* **1997**, *119*, 11104–11105.
- (10) Van Hardeveld, R.; Hartog, F. *Surf. Sci.* **1969**, *15*, 189–230.
- (11) Duncan, T. M.; Reimer, J. A.; Winslow, P.; Bell, A. T. *J. Catal.* **1985**, *95*, 305–308.
- (12) Seidl, M.; Perdew, J. P.; Brajczewska, M.; Fiokhais, C. *J. Chem. Phys.* **1998**, *108*, 8182–8189.
- (13) Feibelman, P. J.; Hamann, D. R. *Surf. Sci.* **1985**, *149*, 48–66.
- (14) Slichter, C. P. *Principles of Magnetic Resonance*, 3rd enlarged and updated ed.; Springer-Verlag: 1990; Vol. 1.
- (15) Atkins, P. *Physical Chemistry*, 6th ed.; W. H. Freeman and Company: New York, 1998.

JA028302J